A Novel Method for Turn-to-Turn Fault Protection of Generator Stators and Rotors

B. Kasztenny, N. Fischer, and D. Taylor
Schweitzer Engineering Laboratories, Inc.

Presented at the
13th International Conference on Developments in Power System Protection
Edinburgh, United Kingdom
March 7–10, 2016

A novel method for turn-to-turn fault protection of generator stators and rotors

B. Kasztenny, N. Fischer, D. Taylor

Schweitzer Engineering Laboratories, Inc., 2350 NE Hopkins Court, Pullman, WA 99163 USA,
normann_fischer@selinc.com

Keywords: Generator protection, differential protection, generator stator faults, generator rotor faults, generator turn-to-turn faults.

Abstract

This paper proposes a new principle for generator turn-to-turn fault protection based on the ampere-turn balance between the stator negative-sequence current and the double-frequency component of the field current. The paper describes two protection elements using this principle: a stator-rotor current unbalance element that uses the current magnitudes and a stator-rotor current differential element that uses the current phasors. The paper derives the new methods, discusses their dependability, sensitivity, and security, and illustrates their operation with computer simulations and test results from a physical made-to-scale generator.

1 Introduction

Stator differential protection, either per-phase or negative-sequence, does not detect turn-to-turn faults in generator stators because these faults do not upset Kirchhoff's current balance between the terminal and neutral-side stator currents. Split-phase protection is the traditional solution for detecting turn-to-turn faults in large hydroelectric generators with split windings [1]. In other types of generators, the stator is often left unprotected against turn-to-turn faults. This paper shows that applying the ampere-turn (AT) balance principle between the negative-sequence current (I_2) in the stator and the double-frequency component in the field current (I_F) of the generator provides turn-to-turn fault protection for both the stator and rotor. Based on this principle, the paper proposes two new protection elements: the stator-rotor current unbalance (60SF) element, which balances the magnitude of I_2 with the properly ratio-matched magnitude of the double-frequency component in I_F, and the stator-rotor current differential (87SF) element, which uses the generator stator and rotor current phasors. The paper derives the new elements and illustrates their operation using computer simulations and tests from a made-to-scale generator. We give a more comprehensive discussion in [2].

2 Stator-rotor-bound protection

With reference to Fig. 1, we can think of a generator as a rotating transformer with an equivalent positive-sequence winding and current (I_1), a negative-sequence winding and current, a field winding and current, and a damper winding, if present. The stator I_2 creates a rotating magnetic field in the opposite direction of the rotor rotation (both the rotor and the magnetic field rotate at a speed corresponding to the power system frequency (ω)). As a result, I_2 induces a double-frequency (2ω) current in the field winding and other parts of the rotor, including the damper windings (if present) and the rotor core surface.

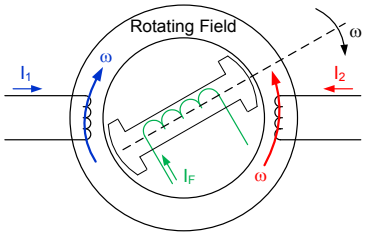

Fig. 1. The negative-sequence stator current induces double-frequency currents on the field and damper windings.

We combine the double-frequency currents flowing in other parts of the rotor into one current, called the damper current, which flows in an equivalent damper winding. When looking at the generator from the stator side and considering I_2, we can view the generator as a three-winding rotating transformer, having the stator winding fed with I_2, and the damper and field winding fed with a double-frequency current as depicted in Fig. 2a. We can provide turn-to-turn fault protection for the stator and rotor of a generator by applying the AT balance to the equivalent three-winding transformer in Fig. 2a.

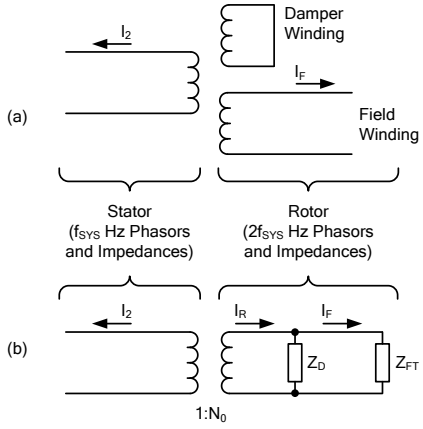

Fig. 2. An equivalent three-winding transformer relating the stator I_2 and the double-frequency components of the field and damper currents (a); two-winding representation with the field and damper windings on the same voltage base (b).

We can measure the stator I_2 and the double-frequency current component of the field. However, we are not able to measure the damper winding current. We can overcome this obstacle by examining Fig. 2b, in which we convert the damper and field impedances to the same voltage base and connect the two circuits in parallel to form a single equivalent winding. This way, we reduce the three-winding transformer to an equivalent two-winding transformer. Assuming the exciter does not generate any significant double-frequency voltage, the field winding can be considered shorted with the total impedance of the field winding and the exciter circuit, Z_{FT}. Z_D is the damper winding leakage impedance. The Z_D and Z_{FT} impedances are double-frequency impedances brought to the same voltage base. Fig. 2b shows that we can provide turn-to-turn fault protection by applying the AT balance between I_2 in the stator and the total rotor current (I_R). Again, we cannot measure I_R. However, as long as Z_D and Z_{FT} are constant, we can calculate I_R from the measured I_F:

$$I_R = I_F \bullet \left(1 + \frac{Z_{FT}}{Z_D}\right) \tag{1}$$

The currents and impedances in (1) are double-frequency quantities. Assuming the turns ratio of the equivalent two-winding transformer is N_0, the AT balance condition for any external unbalance in a healthy generator is:

$$I_2 = N_0 \bullet I_R = N_0 \bullet I_F \bullet \left(1 + \frac{Z_{FT}}{Z_D}\right) \tag{2}$$

Therefore, for any external unbalance, including faults, the ratio N_{SF} of the magnitudes of I_2 and the double-frequency field current for a healthy generator is:

$$N_{SF} = \left|\frac{I_2}{I_F}\right| = N_0 \bullet \left|1 + \frac{Z_{FT}}{Z_D}\right| \tag{3}$$

A turn-to-turn fault in the rotor or stator will upset the AT balance conditions (2) and (3), which allows the detection of such faults. To test this hypothesis, we simulated external faults and internal turn-to-turn faults in a sample 200 MW, 13.8 kV, 60 Hz generator using a Real Time Digital Simulator (RTDS®) [2], [3]. Fig. 3 shows the terminal voltages and currents for an external phase-to-phase fault at the system side of the generator step-up transformer. Fig. 4 shows voltages and currents for a 5 percent turn-to-turn fault while the generator was loaded at 200 MW. A 5 percent turn-to-turn fault is the lowest percentage turn-to-turn fault that can be presently modeled in the RTDS [3]. Fig. 5 shows the magnitudes of currents I_2 and I_F and their ratio for the external fault case of Fig. 3. The I_2/I_F magnitude ratio settles at a value of approximately 13.4 for this external unbalance. The 13.4 ratio for this particular generator should apply for any external unbalance condition. We tested this premise by simulating a number of external unbalanced faults with the I_2 magnitude varying between 175 A and about 17 kA. Fig. 6 shows these external faults as dots on the I_2 versus I_F current magnitude plane. As we can see, all the external fault cases plot as a straight line with a slope of 13.4. Having concluded that the I_2/I_F magnitude ratio holds constant for external faults, we now direct our attention to turn-to-turn faults. Fig. 7 shows the key signals for the simulated 5 percent turn-to-turn fault of Fig. 4.

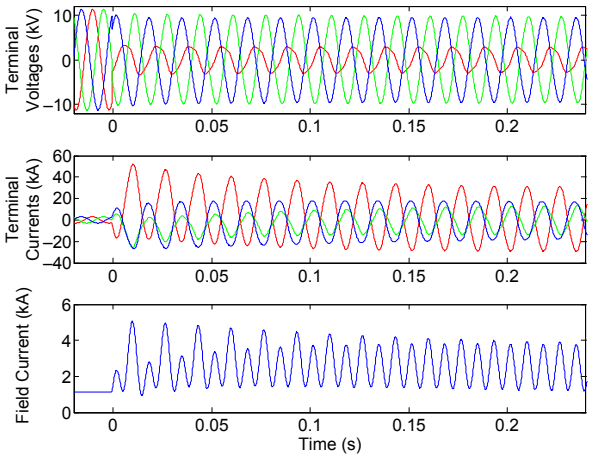

Fig. 3. External fault: terminal voltages and currents and field current.

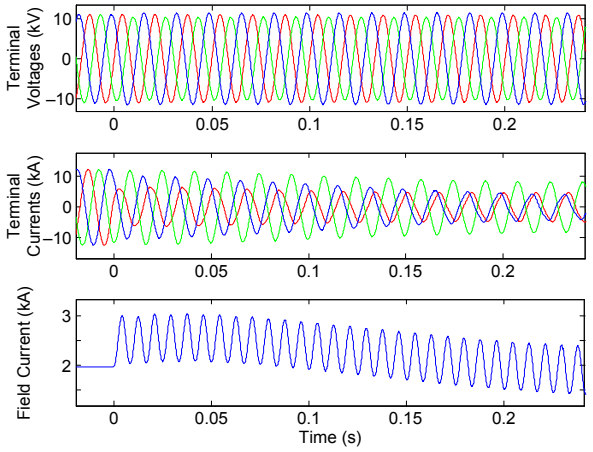

Fig. 4. Turn-to-turn fault: terminal voltages and currents and field current.

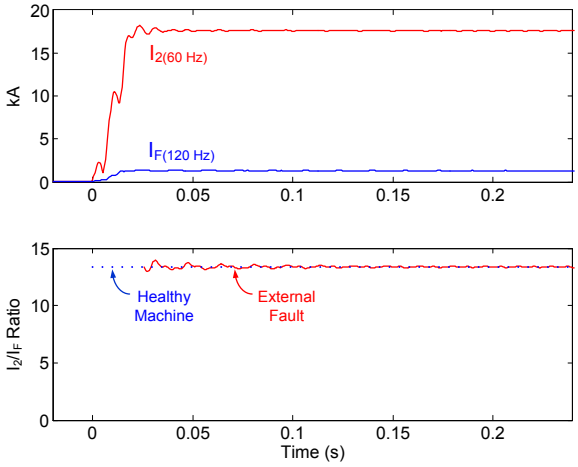

Fig. 5. External fault of Fig. 3: I_2 magnitude (60 Hz), I_F magnitude (120 Hz), and magnitude ratio.

Note that for this fault, the I_2/I_F magnitude ratio is about 6 compared with 13.4 for a healthy generator. Such a significant difference allows us to detect this turn-to-turn fault very reliably.

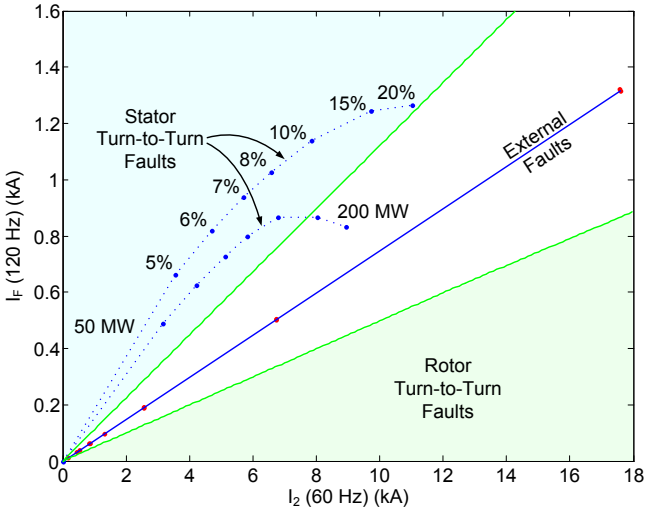

Fig. 6. I_2 magnitude versus double-frequency I_F magnitude for external faults and turn-to-turn faults.

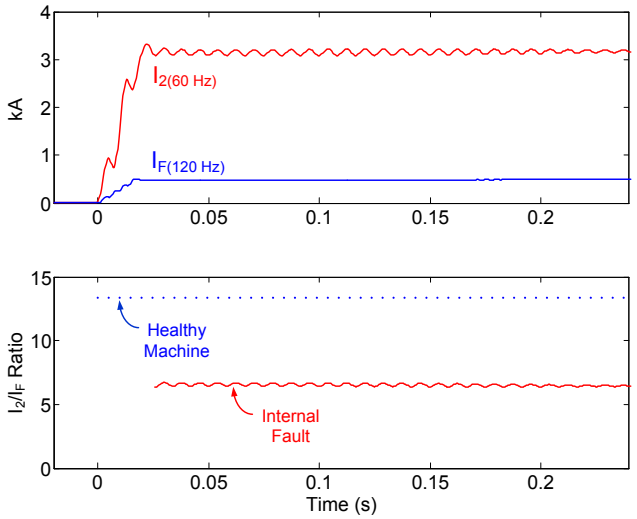

Fig. 7. Turn-to-turn fault of Fig. 4: I_2 magnitude (60 Hz), I_F magnitude (120 Hz), and magnitude ratio.

Fig. 6 shows the plot of a number of turn-to-turn faults on the I_2 versus I_F current magnitude plane for generator loads of 50 MW and 200 MW. As we can see, these faults are located away from the external faults line. The measured magnitude of I_F depends on the generator loading and is higher for a lightly loaded generator. Even for a fully loaded generator, the I_2/I_F magnitude ratio for turn-to-turn faults involving less than 10 percent of the turns differs by about 100 percent compared with the healthy generator. For faults involving 20 percent or more of the turns, the ratio is a less effective decision factor, but these faults are very unlikely.

Note that the 5 percent turn-to-turn faults plot a considerable distance from the line of external faults. We know that for turn-to-turn faults approaching 0 percent of shorted turns, there is no negative-sequence current in the stator or double-frequency current in the field winding. Therefore, we can extrapolate the dashed lines in Fig. 6 toward the origin of the plot. By doing so, we can see that the outlined principle will work well for turn-to-turn faults involving much less than 5 percent of the turns (the RTDS model we used is limited to 5 percent of the turns for a turn-to-turn fault [3]). The physical model testing results described in Section 5 confirm this hypothesis about faults with very few turns.

3 Stator-rotor current unbalance element

Based on the principle derived above, we propose a new protection element: the stator-rotor current unbalance (60SF) element. As shown in Fig. 8, the relay measures the stator currents to calculate the negative-sequence stator current magnitude. It measures the field current (using a shunt, for example) to calculate the double-frequency field current magnitude.

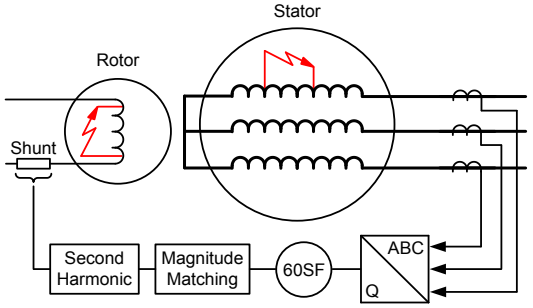

Fig. 8. The 60SF turn-to-turn fault protection element for synchronous generators.

The relay applies the effective transformation ratio (N_{SF}) to match the magnitudes and checks to determine if the two current magnitudes balance. A simple implementation of the 60SF element uses the following operating signal:

$$I_{OP} = \left| \left| I_{2(f_{SYS}\ Hz)} \right| - N_{SF} \bullet \left| I_{F(2f_{SYS}\ Hz)} \right| \right| \qquad (4)$$

and the following restraining signal:

$$I_{RST} = \left| I_{2(f_{SYS}\ Hz)} \right| + N_{SF} \bullet \left| I_{F(2f_{SYS}\ Hz)} \right| \qquad (5)$$

Where: N_{SF} = effective ratio between the two currents for a healthy generator.

f_{SYS} = system frequency.

Comparing the operating signal (4) with a percentage of the restraining signal (5) results in the operating characteristic shown by the green lines in Fig. 6 for a slope setting value of 20 percent. The restraining region is the area between the green lines, and the operating region is the area outside the green lines. The currents involved in (4) and (5) are in primary amperes or properly matched secondary amperes. We calculate the I_2 phasor using a filter tuned at the fundamental system frequency and extract the I_F phasor using a filter tuned at double the system frequency. For accuracy, the two filters process frequency-tracked samples or use an equivalent method to ensure measurement accuracy should the frequency change. In order to illustrate the operation of the 60SF element using (4) and (5), we simulated an external phase-to-phase fault, which evolved into a 5 percent turn-to-turn fault in our sample generator loaded at 100 MW. Fig. 9 shows the terminal voltages and currents and the field current.

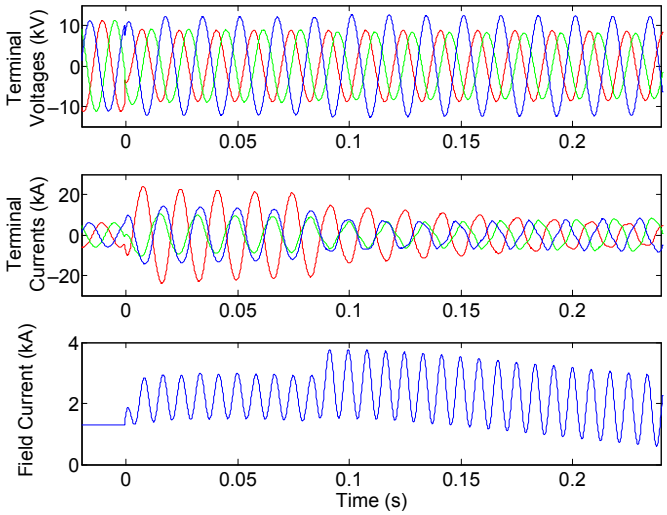

Fig. 9. Evolving external-to-internal fault: terminal voltages and currents and field current.

Fig. 10 shows the I_2 and I_F magnitudes and their ratio.

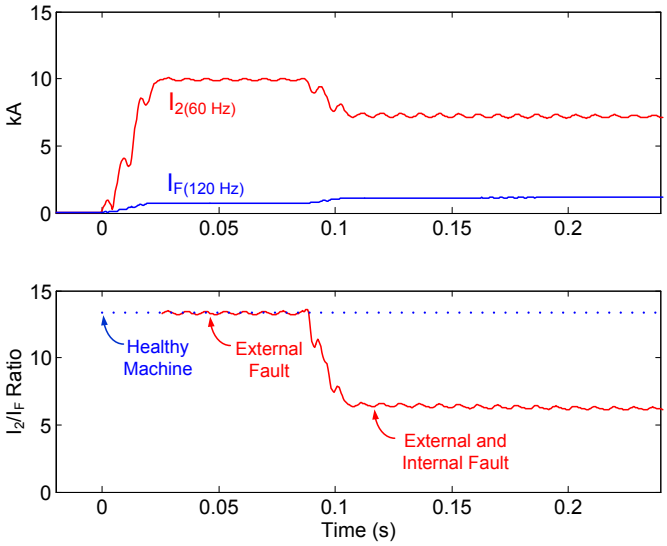

Fig. 10. Evolving external-to-internal fault: I_2 magnitude (60 Hz), I_F magnitude (120 Hz), and their magnitude ratio.

The ratio remains at 13.4 during the external fault as expected and changes dramatically to about 6 when the turn-to-turn fault is simultaneously introduced 5 cycles into the external fault. Fig. 11 shows this case on the operating-restraining current plane per (4) and (5) with a slope setting of 20 percent.

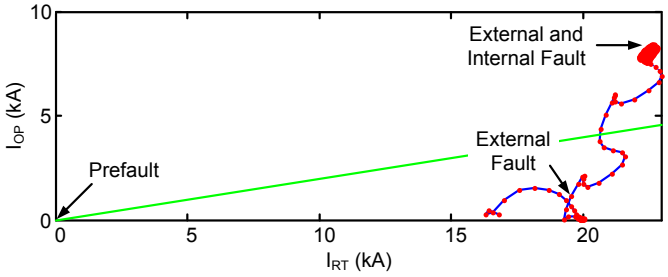

Fig. 11. Evolving external-to-internal fault: fault trajectory on the operating-restraining current plane per (4) and (5).

The trajectory first settles in the restraining region in response to the external fault and moves into the operating region once the internal turn-to-turn fault is introduced.

4 Stator-rotor current differential element

So far, we have only used the magnitudes of the two currents involved in the AT balance between the rotor and stator of the generator. Can we develop a current differential element using the generator stator and rotor current phasors and gain more sensitivity? To develop a phasor-based current differential (87SF) element, we need to solve two challenges:

- The two compared currents are of different frequencies i.e., their phasors rotate at different angular velocities.
- The rotor position with respect to the stator is load dependent.

We solve the first challenge by slowing down the field current double-frequency phasor by dividing it by a unity vector that rotates at the system frequency. One simple implementation of this principle is to use the positive-sequence voltage phasor (V_1) as follows:

$$I_{F(f_{SYS}\ Hz)} = I_{F(2f_{SYS}\ Hz)} \bullet \frac{|V_1|}{V_1} \tag{6}$$

The advantages of using (6) are that we do not need to use the frequency explicitly and the calculation is correct even as the frequency changes during faults. For the second challenge, our simulations show that to ensure proper phase relationships between the two compared currents for external unbalances, we need to shift the field current given by (6) by the following angle:

$$\Theta_C = \angle\left(\frac{E_{qPRE}}{V_{1PRE}}\right) + \frac{\pi}{2} \tag{7}$$

$$E_{qPRE} = V_{1PRE} + jX_d \bullet I_{1PRE} \tag{8}$$

Where: V_{1PRE} = predisturbance V_1.

I_{1PRE} = predisturbance I_1.

X_d = generator direct axis reactance.

In other words, when using V_1 for demodulation in (6), we need to rotate the current by the angle between V_1 and E_d. This angle equals the angle between V_1 and E_q plus 90 degrees per (7) and (8). We can further combine (7) and (8) and use:

$$\Theta_C = \angle\left(\frac{j \bullet V_{1PRE} - X_d \bullet I_{1PRE}}{V_{1PRE}}\right) \tag{9}$$

In order to be able to use (6) and (9), we need to use voltage signals in the 87SF element in addition to the current signals and we must capture the prefault values of the stator voltages and currents. We also need to know the generator direct axis reactance. These requirements make the 87SF element more advanced than the simpler 60SF element. Fig. 12 shows the properly aligned currents for the evolving fault case of Fig. 9.

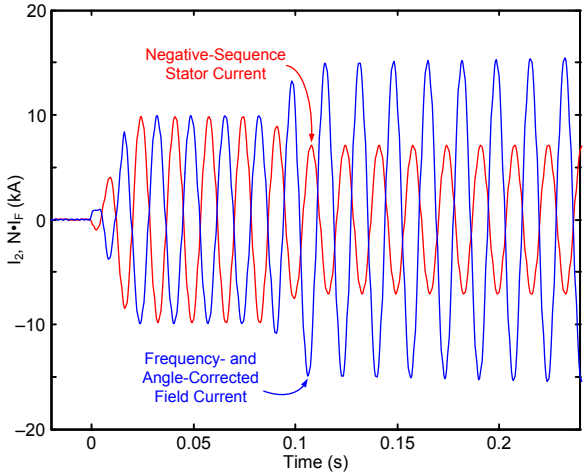

Fig. 12. Evolving external-to-internal fault: I_2, and frequency-matched and angle-corrected I_F.

As expected, the two currents are equal in magnitude and out of phase for the external fault. Once the internal turn-to-turn fault occurs 5 cycles into the external fault, the magnitudes no longer match and the phases shift, allowing for a more sensitive fault detection. A simple implementation of the 87SF element uses the following differential signal:

$$I_{DIF} = \left| I_{2(f_{SYS}\ Hz)} + N_{SF} \bullet I_{F(f_{SYS}\ Hz)} \bullet 1\angle -\Theta_C \right| \qquad (10)$$

and the following restraining signal:

$$I_{RST} = \left| I_{2(f_{SYS}\ Hz)} - N_{SF} \bullet I_{F(f_{SYS}\ Hz)} \bullet 1\angle -\Theta_C \right| \qquad (11)$$

Comparing the operating and restraining signals (10) and (11) in a slope equation results in a typical percentage differential characteristic. Fig. 13 shows the block diagram of the 87SF element.

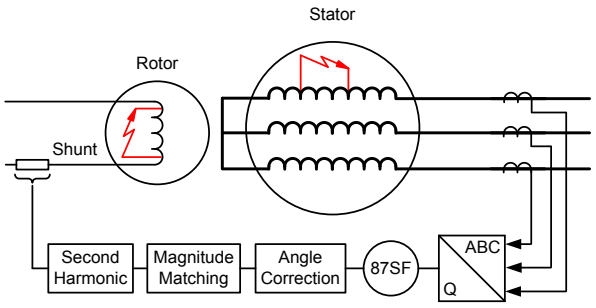

Fig. 13. The 87SF turn-to-turn fault protection element for synchronous generators.

Fig. 14 shows a trajectory of the evolving fault of Fig. 9 on the differential-restraining plane per (10) and (11) with a 20 percent slope setting. When the external fault occurs, the restraining signal increases to about 20 kA while the differential signal is very low. When the turn-to-turn fault occurs after 5 cycles, the differential signal increases to about 8 kA, yielding a reliable operation for this 5 percent turn-to-turn fault, despite the simultaneous external fault. Comparing Fig. 11 (60SF) and Fig. 14 (87SF), we conclude that the two elements behave in a similar fashion, with the 87SF element having a slightly higher operating signal. This is because the phase angle between the two currents does not change much for this turn-to-turn fault (Fig. 12).

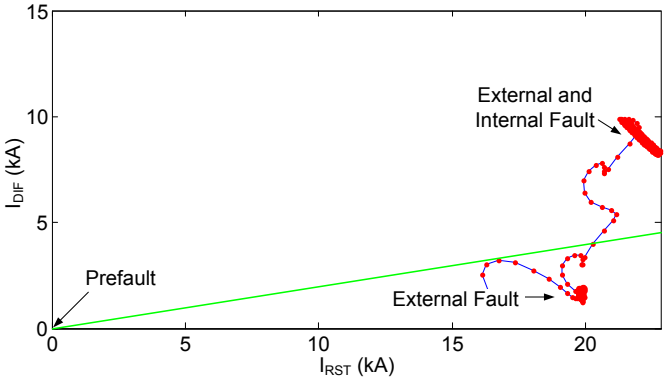

Fig. 14. Evolving external-to-internal fault: fault trajectory on the differential-restraining current plane per (10) and (11).

If the phase angle changed more, the operating signal of the 87SF element would be even higher than that of the 60SF element. According to our simulations, differences in favor of the 87SF element are more visible for turn-to-turn faults on a heavily loaded generator.

5 Physical model testing results

We tested the described protection elements using a three-phase 20 kVA, 220 V, 60 Hz, three-pole laboratory generator driven by an induction motor. The generator stator has 54 slots and two 100-turn windings per phase, with a 14/18 pitch. The windings have taps that allow applying 1, 2, 3, 5, and 10 percent turn-to-turn faults. Fig. 15 shows terminal voltages and currents, as well as the field current, for an external phase-to-phase fault at the laboratory generator terminals.

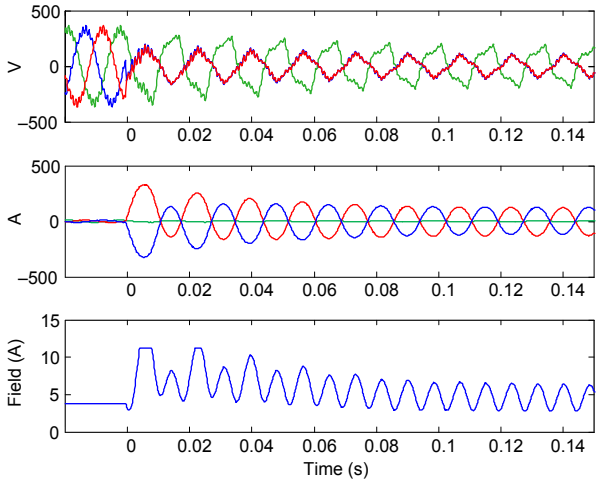

Fig. 15. External fault for the laboratory generator: terminal voltages and currents and field current.

Fig. 16 shows the magnitudes of currents I_2 and I_F and their ratio for the external fault case of Fig. 15. The I_2/I_F magnitude ratio settles at about 40. We obtained similar results for external single-phase-to-ground faults. We applied 1, 2, 3, 5, and 10 percent turn-to-turn faults at the laboratory generator stator. Fig. 17 shows a 3 percent turn-to-turn fault. Fig. 18 shows the signals for the 3 percent turn-to-turn fault of Fig. 17.

For this fault, the I_2/I_F magnitude ratio is about 50 (compared with 40 for a healthy generator). This difference allows us to detect this turn-to-turn fault very reliably. We obtained similar results for the other turn-to-turn faults, including the 1 percent fault, which is a single-turn fault at the 100-turn stator winding.

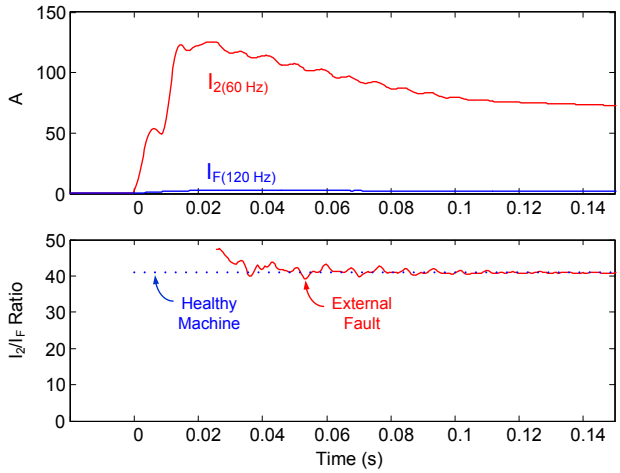

Fig. 16. External fault of Fig. 15: I_2 current magnitude (60 Hz), I_F magnitude (120 Hz), and magnitude ratio

For internal turn-to-turn fault testing, we synchronized the laboratory generator to the laboratory system grid to provide an external power source that injects negative-sequence current to the generator stator windings. As mentioned earlier, an induction motor drives the synchronous generator. The problem with this setup is that as the output of the generator increases, the slip of the induction motor increases, which causes the synchronous speed of the generator to decrease (the generator frequency decreases from nominal). Hence, when the laboratory generator is synchronized to the local power system, it operates at the system frequency, which results in the synchronous generator functioning as a synchronous condenser and not delivering any active power to the power system. The generator stator current is extremely small and heavily distorted for this operating condition, as shown in Fig. 17.

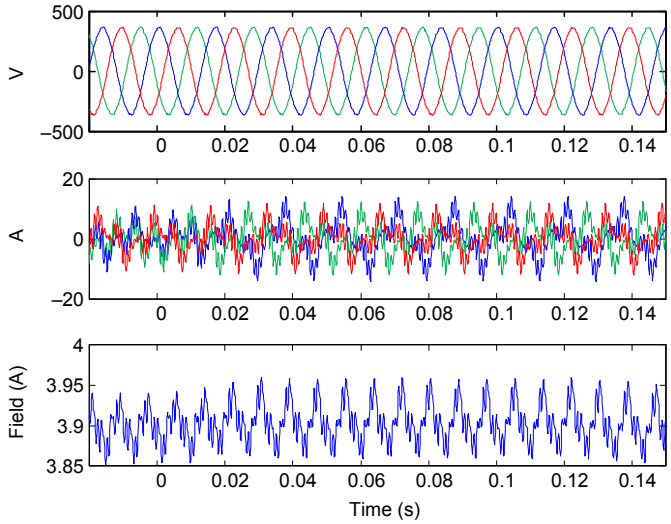

Fig. 17. Turn-to-turn fault at the laboratory generator stator: terminal voltages and currents and field current.

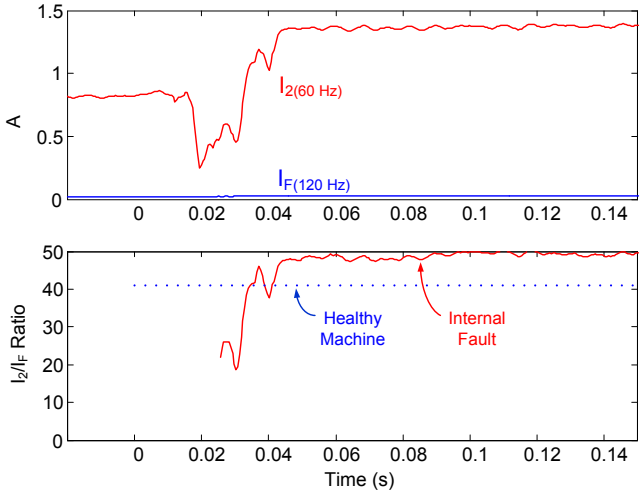

Fig. 18. Turn-to-turn fault of Fig. 17: I_2 magnitude (60 Hz), I_F (120 Hz), and magnitude ratio.

6 Conclusion

This paper derives and explains two novel protection elements for generator turn-to-turn fault protection: 60SF and 87SF. These elements are based on the AT balance between the stator negative-sequence current and the rotor double-frequency current. The elements do not require the damper winding currents to be measured and therefore can be practically applied as long as the impedances of the field and damper windings are constant.

7 References

[1] IEEE Standard C37.102, IEEE Guide for AC Generator Protection.

[2] B. Kasztenny, N. Fischer, and H. J. Altuve, "Negative-Sequence Differential Protection—Principles, Sensitivity, and Security," proceedings of the 41st Annual Western Protective Relay Conference, Spokane, WA, October 2014.

[3] A. B. Dehkordi, A. M. Gole, and T. L. Maguire, "Real Time Simulation of Internal Faults in Synchronous Generators," proceedings of the 7th International Conference on Power System Transients, Lyon, France, June 2007.